Available online at www.sciencedirect.com
ScienceDirect
Trans. Nonferrous Met. Soc. China 34(2024) 2686−2701
Transactions of Nonferrous Metals Society of China
www.tnmsc.cn

Separation of halogens and recovery of heavy metals from secondary copper smelting dust

Zhi-lou LIU[1], Zhi-kang CHEN[1], Fu-ze SUN[1], Zhi-heng ZHANG[1], Kang YAN[1], Shui-ping ZHONG[1], Hui LIU[1], Rui-xiang WANG[1], Jia-yuan LI[2], Zhi-feng XU[3,4]

1. School of Metallurgy Engineering, Jiangxi University of Science and Technology, Ganzhou 341000, China;
2. School of Chemistry and Environmental Science, Xiangnan University, Chenzhou 423000, China;
3. Ganzhou Engineering Technology Research Centre of Green Metallurgy and Process Intensification, Ganzhou 341000, China;
4. Key Laboratory of Ionic Rare Earth Resources and Environment, Ministry of Natural Resources, Ganzhou 341000, China

Received 1 March 2023; accepted 12 October 2023

Abstract: The separation of halogens and recovery of heavy metals from secondary copper smelting (SCS) dust using a sulfating roasting−water leaching process were investigated. The thermodynamic analysis results confirm the feasibility of the phase transformation to metal sulfates and to gaseous HF and HCl. Under the sulfating roasting conditions of the roasting temperature of 250 °C and the sulfuric acid excess coefficient of 1.8, over 74 wt.% of F and 98 wt.% of Cl were volatilized into flue gas. Approximately 98.6 wt.% of Zn and 96.5 wt.% of Cu in the roasting product were dissolved into the leaching solution after the water leaching process, while the leaching efficiencies of Pb and Sn were only 0.12% and 0.22%, respectively. The mechanism studies indicate the pivotal effect of roasting temperature on the sulphation reactions from various metal species to metal sulfates and the salting out reactions from various metal halides to gaseous hydrogen halides.

Key words: secondary copper smelting dust; sulfating roasting; water leaching; halogen volatilization; heavy metal separation

1 Introduction

With the diminishment of copper mineral resources, copper recovery from secondary copper resources has become an important issue [1−3]. The copper output from secondary copper resources has increased annually in China, accounting for more than 20% of all refined copper output in 2015 [4]. The dominant recovery technology from secondary copper resources is pyrometallurgical reduction smelting using coke as a reducing agent, which is a flexible and effective technique for handling copper materials with a low grade and a high impurity. However, the formation of secondary copper smelting (SCS) dust is inevitable during the high-temperature reduction smelting process. This dust usually contains high levels of valuable heavy metals and harmful halogens [5−7]. For example, CHEN et al [8] reported that the mass fractions of Pb and Cl in secondary copper smelting dust may be as high as 45.69% and 18.90%, respectively. Therefore, developing a recycling technique to recover resources and reduce environmental risk is

Corresponding author: Rui-xiang WANG, Tel: +86-13607974010, E-mail: wrx9022@163.com;
Jia-yuan LI, Tel: +86-15096100608, E-mail: 422598128@qq.com
DOI: 10.1016/S1003-6326(24)66569-6

of great significance [9].

Currently, two mainstream categories for the cyclic utilization of smelting dust are hydrometallurgical process and pyrometallurgical process. Many studies have reported various hydrometallurgical processes, including acid leaching [10], alkaline leaching [11,12], pressure leaching [13,14] and bioleaching [15], to extract valuable heavy metals. After the leaching process, the dissolved metal is recycled through the cementation [16], precipitation [17,18], solvent extraction [19], or electrolysis [20,21]. Additionally, the pyrometallurgical processes [22−25], such as carbothermal reduction, have attracted increasing attention due to their high reaction rate, wide adaptability and short flow sheet. However, these methods are unsuitable for the treatment of SCS dust because of abundance of halogens in SCS dust, particularly chlorine. Halogen elements are easily spread in the leaching solution along with valuable metal ions in the hydrometallurgical process, which counteracts the subsequent metal separation and purification steps, such as solvent extraction and electrodeposition. In the pyrometallurgical process, the presence of halogen elements can reduce the metal recovery because of the volatility of metal halides at high temperatures.

A sound strategy for the disposal of halogen-containing dust is the selective separation of halogens before the resource utilization of valuable metals. CHEN et al [26] used water washing to remove soluble chlorine from electric arc furnace dust. However, when the water washing was used to remove halogens from SCS dust, only soluble halides can be leached and some of the toxic metal ions would inevitably enter into the leaching solution, resulting in the low leaching efficiency and heavy metal pollution. The other technique is thermal volatilization at temperatures of greater than 900 °C to ensure the complete volatilization of metal halides [27,28]. The results of a life-cycle assessment confirmed that thermal volatilization to separate halogens was a typical process with a high environmental burden and a low-cost effectiveness [29]. Based on the aforementioned analysis, developing an appropriate approach that can achieve the dual purposes of halogen separation and resource recycling is still challenging.

In this study, a technology using a two-step process including sulfating roasting and water leaching was innovatively developed to separate halogens and recover valuable metals from SCS dust. In brief, various metal species in the SCS dust were transformed to metal sulfates in the sulfating roasting step, and the halogen elements were simultaneously removed in the form of gaseous halogen hydrides. The Zn and Cu in the roasting product were separated from Pb and Sn in the following water leaching step. To validate these results, the effects of some critical parameters were comprehensively evaluated. The metal recovery and halogen separation mechanisms were also explored. The results not only strongly support the clean utilization of SCS dust, but also provide a deep insight into species transformation rule in the sulfating roasting process.

2 Experimental

2.1 Materials

All chemical reagents including concentrated sulfuric acid (H_2SO_4, 98 wt.%), and sodium hydroxide (NaOH) were analytically pure and obtained from Sinopharm Chemical Reagent Co., Ltd. The SCS dust used in this study was obtained from a secondary copper smelter in Jiangxi, China, and was collected from the reduction smelting process. Before each experiment, the collected SCS dust was dried at 80 °C for 24 h in an air-dry oven to remove the moisture. All chemical reagents were used without further purification.

2.2 Experimental apparatus and procedure

A lab-scale apparatus was set up to evaluate the sulfating roasting process, and a schematic diagram is shown in Fig. S1 of Supplementary Materials. High purity nitrogen and oxygen were used to simulate the reaction atmosphere, and the corresponding flue gas components were controlled by changing the flow of oxygen. The total flow rate was fixed at 0.5 L/min in all experiments. A tube furnace (OTF−1200X-S, Kejing, China) was applied to controlling the reaction temperature, and the generated hydrogen halide gas was continuously removed to the downstream tail gas absorption system. The acid gas in the tail gas, including HCl and SO_2, was absorbed by an enough sodium hydroxide solution.

Before each experiment, the simulated flue gas was pumped for at least 5 min to exhaust the air in

the tube furnace. Then, 10 g of SCS dust was mixed with a certain amount of concentrated sulfuric acid, and the obtained mixture was instantly added to a corundum crucible with a lid. The crucible was placed in the middle of the tube furnace and heated for a fixed period at a set temperature (the temperature error was less than ±5 °C). The roasting product was cooled naturally to room temperature. Each batch of roasting product was leached using 80 mL of pure water at room temperature for 30 min. The stirring rate was 500 r/min for all leaching experiments. Then, the liquid−solid mixture was filtered to obtain the leaching solution and residue. The experimental details of extraction and reduction were presented in the Section 1 of Supplementary Materials. The separation efficiencies (E) of heavy metals and halogens after the sulfating roasting−water leaching process were calculated using Eqs. (1)−(3):

$$E_{(\mathrm{Cu,Zn})}=\frac{C_1V_1}{10w_0} \tag{1}$$

$$E_{(\mathrm{Pb,Sn})}=100\%-\frac{w_1M}{10w_0} \tag{2}$$

$$E_{(\mathrm{F,Cl})}=\frac{C_2V_2}{10w_0} \tag{3}$$

where w_0 represents the mass fraction (wt.%) of Zn, Pb, Cu, Sn, F and Cl in the SCS dust; 10 represents the mass (g) of SCS dust used in this study (precision of 0.001 g); C_1 and V_1 represent the concentration (g/L) of Zn and Cu in the leaching solution and the total volume (L) of the leaching solution, respectively; w_1 is the mass fraction (wt.%) of Pb or Zn in the residue after water leaching, M represents the total mass (g) of the water leaching residue; C_2 and V_2 are the concentration (mg/L) of F and Cl in the absorption liquid and the total volume (L) of the absorption liquid, respectively.

2.3 Characterization method

The metal element composition in solid samples was confirmed using an inductively coupled plasma optical emission spectrometer (ICP-OES, PerkinElmer, 7300 DV), and the mass fraction of total sulfur was determined by the gravimetric method ($BaSO_4$). The crystal structures of solid samples were measured using X-ray diffraction (XRD, Rigaku, TTRAXIII). The halogen in the SCS dust was extracted according to the Japanese Industry Standard, and the fluorine and chlorine concentrations in the extracting solution were measured using ion chromategraphy (IC, Metrohm, 883IC) [30]. The surface composition and valence states of solid samples were determined by X-ray photoelectron spectroscopy (XPS, Escalab, 250Xi) with Al K_α X-ray (excitation energy of 1486.58 eV) as the excitation source. The binding energies of all the elements were calibrated using the C 1s peak at 284.8 eV. The morphology and elemental distribution of solid samples were analyzed using a field-emission scanning electron microscope (FE-SEM, Nova, NanoSEM 450) equipped with an energy dispersive spectroscopy instrument (EDS, Thermo, NS7). A laser particle sizer (Mastersizer 3000) was applied to determining the particle size distribution of the SCS dust. Raman spectrum analysis (RENISHAW-inVia, USA) was conducted with 532 nm radiation from an He−Ne laser with a output power of 0.5 mW and a acquisition time of 75 s. The thermal analysis was performed using a thermogravimetric analysis instrument (TG−DSC, Netzsch, STA 449 F5, Germany) coupled with a quadruple mass spectrometer (MS, QMA 400). The detailed information for the determination of halogen, XPS and TGA−DSC−MS is described in the Supplementary Materials.

3 Results and discussion

3.1 Characterization of secondary copper smelting dust

The compositions of the main chemical elements in the SCS dust are listed in Table 1. The valuable metal elements are Zn, Pb, Sn and Cu, with corresponding mass fractions of 27.52%, 25.20%, 4.12% and 3.04%, respectively. In addition, some alkali metal elements, such as Na and K, also exist. The nonmetal elements in the SCS dust are mainly Cl and S. A small quantity of fluorine also exists in the SCS dust, which accounts for approximately 0.77% of the total mass. Notably, the chlorine content is as high as 9.75%. The contents of heavy metals in the SCS dust are apparently higher than those in primary metal mines [31]. Therefore, the recovery of heavy metals from SCS dust is very important.

The results in Fig. 1(a) indicate a broad grain size distribution, mainly presenting two regions

at approximately 180 nm and 3 μm, respectively. The cumulative volume distribution data show that a particle size proportion of less than 300 nm accounts for over 40% of the total volume, indicating the inherent feature of the fine particle size of the SCS dust.

The XRD pattern shown in Fig. 1(b) reveals the main phase composition of zincite (ZnO), cotunnite ($PbCl_2$) and metallic lead (Pb), along with small portions of sphalerite (ZnS), teallite ($PbSnS_3$), nantokite (CuCl) and tin chloride ($SnCl_2$). Because the SCS dust used in this study was obtained from the reduction process, some elements, such as zinc, lead and chlorine, easily volatilized into flue gas in the form of metals or compounds. The XRD results indicate that heavy metals primarily exist in the form of insoluble compounds. Therefore, the development of a suitable strategy to ensure the efficient recovery of heavy metals is valuable.

Figure 1(c) displays the SEM morphology and scanning maps of the SCS dust. The SCS dust is mainly composed of fine spherical and flake particles. The particle sizes of the spherical and flake particles are less than 0.5 and 2.5 μm, respectively. The EDS scanning maps of the elemental distribution in Fig. 1(c) reveal the existence of Pb, Sn, Cu, Zn, S, F and Cl elements throughout the analyzed area, suggesting the presence of valuable metals and harmful halogens in the SCS dust. These EDS results are consistent with the XPS results in Fig. S2 of Supplementary Materials.

Table 1 Chemical element analysis results of valuable metals and hazardous halogens in SCS dust, roasting product and leaching residue (wt.%)

Sample	Cu	Zn	Pb	Sn	Na	K	S	F	Cl	Others
SCS dust	3.04	27.52	25.20	4.12	7.01	2.24	2.97	0.77	9.75	17.38
Roasting product	2.14	16.67	13.82	1.93	3.24	1.13	32.72	0.06	0.01	28.28
Leaching residue	0.22	0.46	36.7	5.92	<0.01	<0.01	15.91	0.12	0.01	<40.66

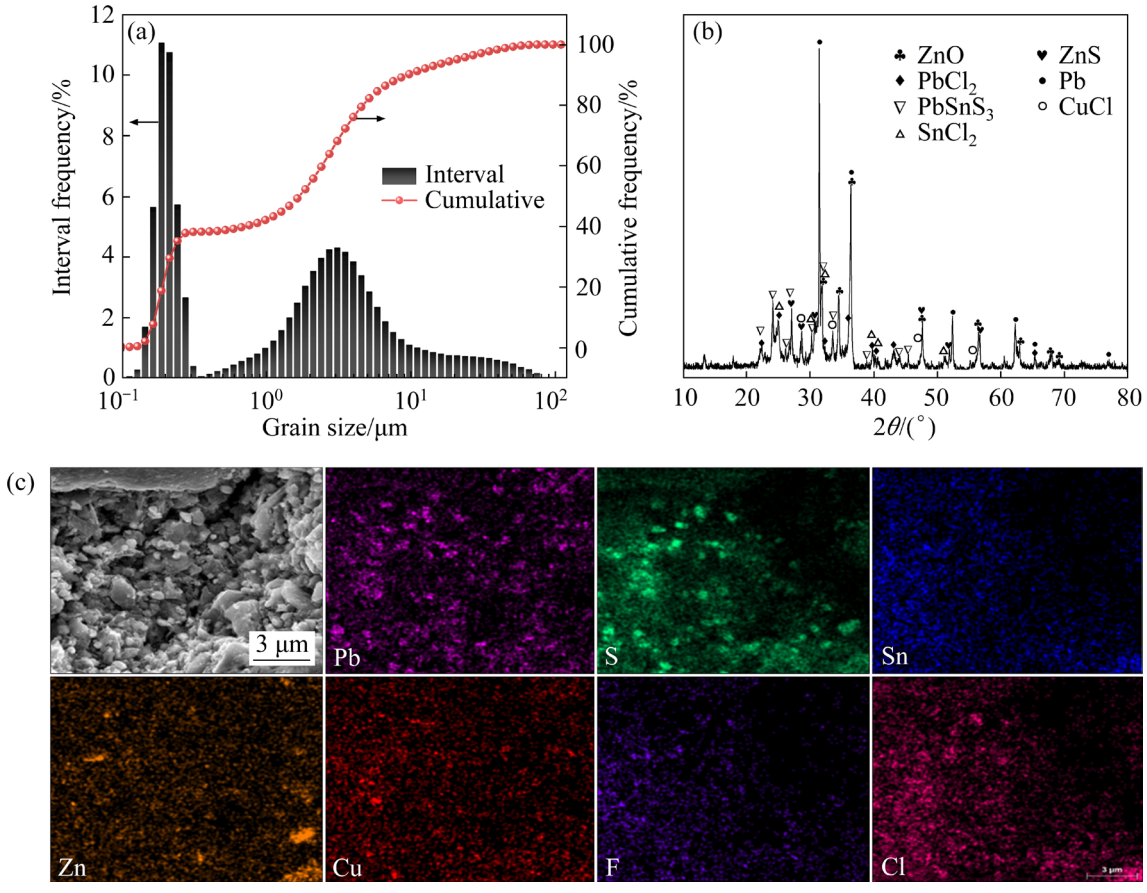

Fig. 1 Particle size distribution (a), XRD pattern (b), and SEM morphology and EDS scanning maps (c) of SCS dust

3.2 Thermodynamic analysis results of roasting process

The transformation behaviour of different compounds in the sulfating roasting process is very important for the recovery of heavy metals and the separation of harmful halogens. Combined with the results from the aforementioned analysis of the main existing species of metal and halogen compounds in the SCS dust, possible chemical reactions with H_2SO_4 are presented in Table 2. Meanwhile, the standard Gibbs free energy (ΔG^{Θ}) at different temperatures was calculated using HSC Chemistry 7.1 software, and the corresponding results are shown in Fig. 2.

Table 2 Possible chemical reactions in sulfating roasting process (The standard state of H_2SO_4 is liquid (l) and gaseous (g) before and after 337 °C, respectively)

No.	Chemical reaction
1	$ZnO+H_2SO_4(l, g)=ZnSO_4+H_2O(g)$
2	$1/4ZnS+H_2SO_4(l, g)=1/4ZnSO_4+H_2O(g)+SO_2(g)$
3	$ZnCl_2+H_2SO_4(l, g)=ZnSO_4+2HCl(g)$
4	$ZnF_2+H_2SO_4(l, g)=ZnSO_4+2HF(g)$
5	$1/2Pb+H_2SO_4(l, g)=1/2PbSO_4+H_2O(g)+1/2SO_2(g)$
6	$PbO+H_2SO_4(l, g)=PbSO_4+H_2O(g)$
7	$1/3Pb_3O_4+H_2SO_4(l, g)=PbSO_4+H_2O(g)+1/6O_2(g)$
8	$1/4PbS+H_2SO_4(l, g)=1/4PbSO_4+H_2O(g)+SO_2(g)$
9	$PbCl_2+H_2SO_4(l, g)=PbSO_4+2HCl(g)$
10	$PbF_2+H_2SO_4(l, g)=PbSO_4+2HF(g)$
11	$1/2Cu+H_2SO_4(l, g)=1/2CuSO_4+H_2O(g)+SO_2(g)$
12	$1/3Cu_2O+H_2SO_4(l, g)=2/3CuSO_4+H_2O(g)+1/3SO_2(g)$
13	$CuO+H_2SO_4(l, g)=CuSO_4+H_2O(g)$
14	$1/4CuS+H_2SO_4(l, g)=1/4CuSO_4+H_2O(g)+SO_2(g)$
15	$2/3CuCl+H_2SO_4(l, g)=2/3CuSO_4+2/3HCl(g)+1/3SO_2(g)+2/3H_2O(g)$
16	$CuCl_2+H_2SO_4(l, g)=CuSO_4+2HCl(g)$
17	$CuF_2+H_2SO_4(l, g)=CuSO_4+2HF(g)$
18	$1/4Sn+H_2SO_4(l, g)=1/4Sn(SO_4)_2+H_2O(g)+1/2SO_2(g)$
19	$1/3SnO+H_2SO_4(l, g)=1/3Sn(SO_4)_2+H_2O(g)+1/3SO_2(g)$
20	$1/2SnO_2+H_2SO_4(l, g)=1/2Sn(SO_4)_2+H_2O(g)$
21	$1/6SnS+H_2SO_4(l, g)=1/6Sn(SO_4)_2+H_2O(g)+5/6SO_2(g)$
22	$SnCl_2+H_2SO_4(l, g)=SnSO_4+2HCl(g)$
23	$SnF_2+H_2SO_4(l, g)=SnSO_4+2HF(g)$
24	$2NaCl+H_2SO_4(l, g)=Na_2SO_4+2HCl(g)$
25	$2KCl+H_2SO_4(l, g)=K_2SO_4+2HCl(g)$
26	$CaCl_2+H_2SO_4(l, g)=CaSO_4+2HCl(g)$
27	$2NaF+H_2SO_4(l, g)=Na_2SO_4+2HF(g)$
28	$2KF+H_2SO_4(l, g)= K_2SO_4+2HF(g)$
29	$CaF_2+H_2SO_4(l, g)=CaSO_4+2HF(g)$

The ΔG^{Θ} values of the possible reactions for all zinc and lead compounds are negative at normal temperatures, indicating that $ZnSO_4$ and $PbSO_4$ are the final species of zinc and lead, respectively (see Figs. 2(a) and (b)). As shown in Fig. 2(c), elemental copper, copper oxides, copper sulfide and copper fluoride react with H_2SO_4 to form $CuSO_4$ in theory. However, the ΔG^{Θ} of the reaction between H_2SO_4 and CuCl becomes negative only when the temperature is greater than 150 °C. This result implies that the roasting temperature should remain above 150 °C to ensure the efficient dissolution of copper. All the types of tin compounds in the SCS dust, except for SnO_2, react with H_2SO_4 in the temperature range of 100−500 °C (see Fig. 2(d)). Figure S3 in Supplementary Materials indicates that liquid H_2SO_4 volatilized and the gaseous H_2SO_4 decomposed to SO_3 and H_2O at the temperature of greater than 500 °C. Therefore, considering the thermodynamic stability of H_2SO_4, the roasting temperature should be below 400 °C.

Figure 2(e) shows the salting out reactions of alkali metal halides for the volatilization of fluorine and chlorine to produce hydrogen halides in the roasting process. The ΔG^{Θ} values of all salting out reactions in Fig. 2(e) are negative, suggesting that volatilization of HF and HCl spontaneously occurred. Overall, we concluded that the chemical reactions of heavy metals to their respective sulfates and the volatilization of halogens can be simultaneously achieved in the appropriate roasting temperature ranges (150−450 °C).

3.3 Separation indices of heavy metals and halogens

The sulfating roasting process is a feasible technology for halogen separation and metal recovery [32,33]. The heavy metals in the roasting product can be separated based on their solubility differences. Therefore, sulfating roasting−water leaching is an effective method for the disposal of SCS dust. The sulfating roasting step is key compared with the water leaching step. Hence, the effects of the critical parameters in the sulfating roasting step, including the excess coefficient of sulfuric acid, the roasting temperature, the reaction

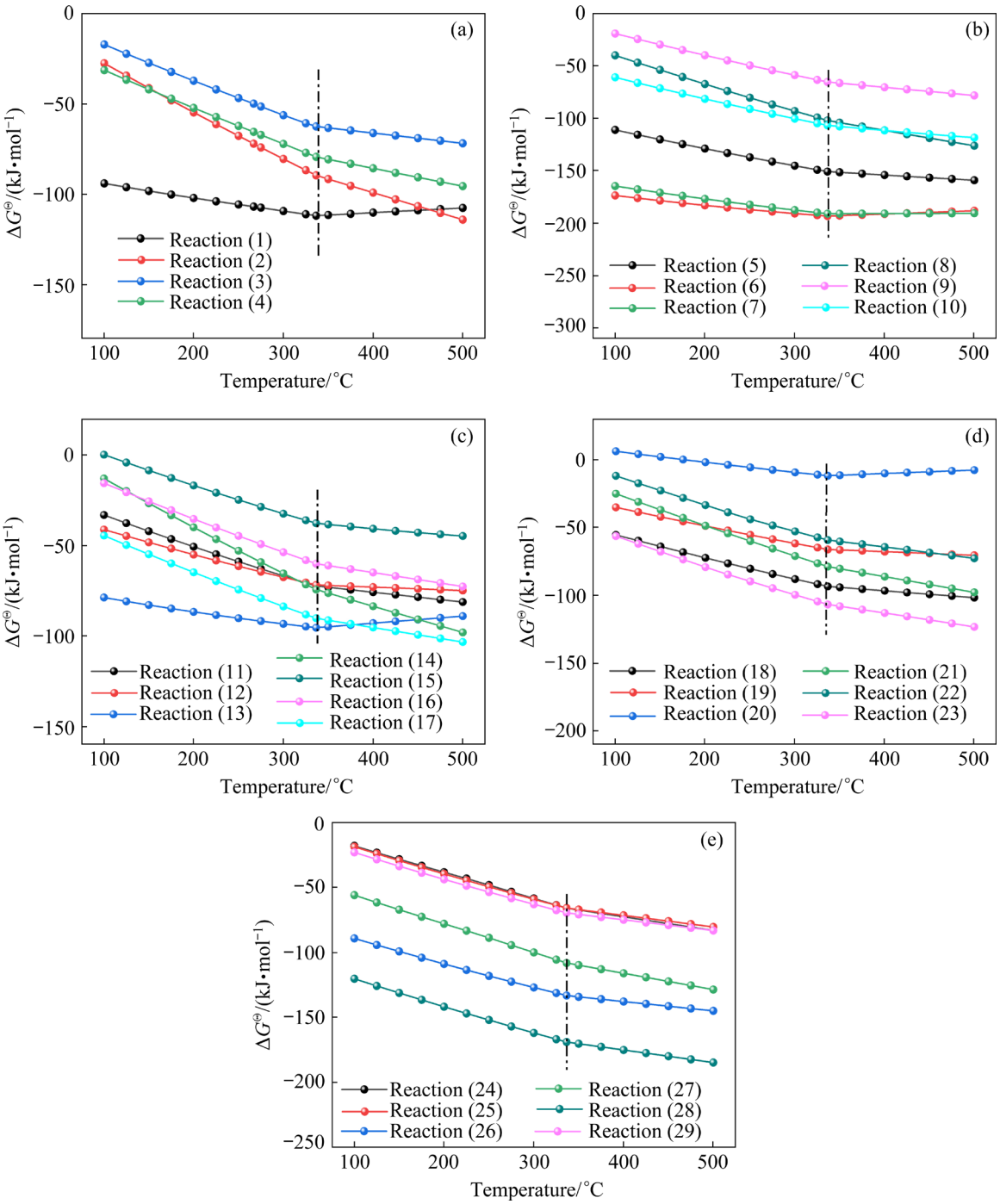

Fig. 2 Thermodynamic diagrams of standard Gibbs free energy ($\Delta G^{\ominus}$) as function of temperature for sulphation reactions of different Zn species (Reactions (1)−(4)) (a), Pb species (Reactions (5)−(10)) (b), Cu species (Reactions (11)−(17)) (c), Sn species (Reactions (18)−(23)) (d) and for salting out reactions of other alkali metal halides (Reactions (24)−(29)) (e)

time and the roasting atmosphere were studied, and the corresponding results are summarized in Fig. 3.

The amount of concentrated sulfuric acid is directly related to the distribution behaviours of valuable metals and the volatilization of halogens. The actual dosage against the theoretical dosage is referred to as the excess coefficient, and the theoretical dosage is 6.6 g/10 g dust according to theoretical calculation. As shown in Fig. 3(a), the leaching efficiencies of Zn and Cu significantly increase as the sulfuric acid excess coefficient increases from 0.8 to 1.6. As the sulfuric acid excess

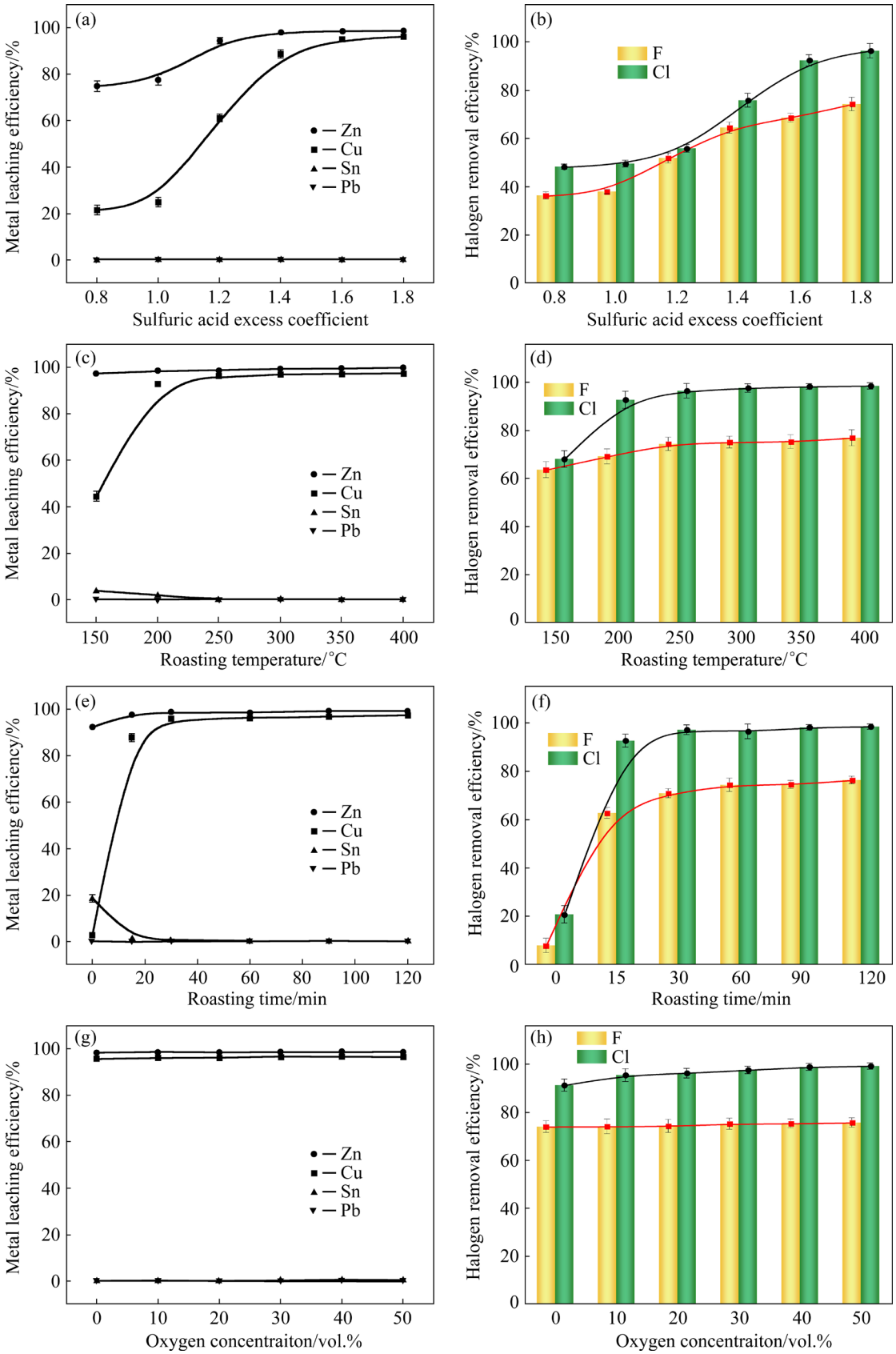

Fig. 3 Effects of sulfuric acid excess coefficient (a, b), roasting temperature (c, d), roasting time (e, f) and oxygen concentration (g, h) on metal leaching efficiency and halogen removal efficiency (Experimental conditions: SCS dust mass 200 g; sulfuric acid excess coefficient 1.6; roasting temperature 250 °C; roasting time 120 min; oxygen concentration 20 vol.%, except when it was a variable)

coefficient increases to 1.6, the corresponding leaching efficiencies of Zn and Cu are more than 98% and 95%, respectively. Pb and Sn are always mainly retained in the leaching residue at any excess coefficient (The specific data of Pb and Sn are supplemented in Table S1 of Supplementary Materials).

Figure 3(b) indicates that the removal of F and Cl significantly depends on the excess coefficient of sulfuric acid, possibly due to the extensive conversion of metal halides in the presence of excessive concentrated sulfuric acid. A high excess coefficient indicates an increase in the amount of residual acid, resulting in a pH decrease of the leaching solution (see Fig. S4 in Supplementary Materials). A low pH will prevent the subsequent extraction and separation of Zn and Cu from the leaching solution. Taking the metal recovery and halogen removal into consideration, the optimal excess coefficient of sulfuric acid is 1.6.

The effect of the roasting temperature on the recovery of heavy metals is shown in Fig. 3(c). At roasting temperatures ranging from 150 to 400 °C, the leaching efficiencies of Zn and Pb were greater than 98% and less than 0.5%, respectively. The leaching efficiency of Cu increased with the roasting temperature in the range of 150−250 °C, but a further increase in the temperature did not promote the leaching of Cu. The thermodynamic calculation shows that the chemical reaction of CuCl oxidation did not occur at room temperature. Combined with the finding that CuCl was the predominant copper phase in the SCS dust, we conclude that a high temperature facilitates the reaction of copper species from insoluble CuCl to dissolvable $CuSO_4$, hence improving the leaching of Cu. A small proportion of Sn, approximately 3.8 wt.%, was dissolved in the solution at a roasting temperature of 150 °C. When the roasting temperature was less than 200 °C, the decomposition of sulfuric acid was incomplete, and the residual sulfuric acid dissolved into solution in the subsequent leaching process, thereby inhibiting the complete hydrolysis reaction of tetravalent tin and leading to the partial dissolution of Sn.

Figure 3(d) displays the volatilization of Cl and F in the sulfating roasting process. Increasing the temperature in the range from 150 to 250 °C facilitated the removal of halogens from the SCS dust, and the removal efficiency exhibited a slight change with a further increase in the temperature. The corresponding removal efficiencies of Cl and F at the optimal temperature of 250 °C are 98.3% and 76.7%, respectively.

The roasting time and reaction atmosphere are two other critical parameters. The roasting time of zero represents the prepared mixture of SCS dust and sulfuric acid. As shown in Fig. 3(e), only a small amount of Cu was leached into solution in the absence of sulfating roasting, and more than 18% Sn was dissolved. This result proves the necessity of sulfating roasting for metals recovery. When the roasting time was increased to 15 min, the leaching efficiency of Cu increased tremendously to higher than 87%, which implies rapid reactions between cuprous chloride and concentrated sulfuric acid. Further increasing the roasting time to over 30 min did not promote the sulphation reaction. Therefore, a roasting time of 30 min is sufficient. The leaching efficiency of heavy metals remained approximately constant as the oxygen concentration changed (see Fig. 3(g)), indicating that sulphation reactions are unrelated to the atmosphere.

As shown in Fig. 3(f), the proportions of removed F and Cl were only 7.68% and 20.54% in the absence of sulfating roasting, respectively. When the roasting time was increased to 15 min, the removal efficiencies of F and Cl increased rapidly to 62.5% and 92.4%, respectively. The roasting time of 30 min is enough for the volatilization of halides produced from salting out reactions. As shown in Fig. 3(h), the volatilization of Cl was slightly improved as the oxygen concentration increased. The fast oxidation and decomposition of metal chloride at high oxygen concentrations may explain why the presence of oxygen facilitates Cl removal. This result indicates that it is unnecessary to control the reaction atmosphere in the actual sulfating roasting process.

3.4 Characteristics of roasting product and leaching residue

Based on the above results, the optimum conditions for the roasting process include a sulfuric acid excess coefficient of 1.6, a roasting temperature of 250 °C, a roasting time of 30 min and an oxygen concentration of 20 vol.%. After sulfating roasting and water leaching, the roasting product and leaching residue were analyzed using XRD, chemical element analysis, SEM and EDS to

further explore the corresponding changes in the mineralogical phases, chemical components, and morphology. As shown in Fig. 4(a) and Table 1, the main phases in the roasting product are zinc sulfate and lead sulfate, and the mass fractions of Zn, Pb and S are 16.67%, 13.82% and 32.72%, respectively. Some weak peaks for copper sulfate and tin sulfate can be observed, and the mass fractions of Cu and Sn in the roasting product are 2.14% and 1.93%, respectively. The phases of zinc and copper sulfate disappeared in the leaching residue (see Fig. 4(b)), consistent with the elemental analysis shown in Table 1. The major chemical components in the leaching residue are Pb, Sn and S, and the corresponding species are insoluble $PbSO_4$ and SnO_2. Tin sulfate is unstable during the leaching process and is easily hydrolyzed to produce stannic oxide. No dust is produced during the sulfating roasting process (see Table S2 in Supplementary Materials). Remarkably, the low concentrations of F and Cl in the roasting product indicate the efficient removal of F and Cl during the roasting process, which is also confirmed by the elemental distribution and balance of F and Cl shown in Table S3 in Supplementary Materials. Notably, the F and Cl concentrations in the tail gas absorption liquid are usually higher than 0.3 and 8.5 g/L respectively, which can be treated using traditional chemical precipitation and evaporative crystallization methods [34,35]. The elemental distribution and balance of F and Cl shown in Table S3 in Supplementary Materials also prove the effective removal of halogens in the sulphating roasting process. The SEM analysis in Fig. 4(c) presents an irregular morphology of the roasting product, which is composed of a bulk porous skeleton and small particles with a diameter of approximately 1 μm. After being leached by water, the porous skeleton disappeared, and the leaching residue exhibited an irregular spherical morphology (see Fig. 4(d)).

3.5 Chemical reaction behaviour during sulfating roasting process

The roasting products obtained at different temperatures and their corresponding leaching residues were characterized using Raman technique to comprehensively elucidate the reaction behaviour during the sulfating roasting process. As shown in Figs. 5(a) and (c), four characteristic peaks, including a v_1 symmetric stretching peak at approximately 980 cm^{-1}, a v_2 symmetric bending peak at approximately 445 cm^{-1}, a v_3 asymmetric stretching peak at approximately 1030 cm^{-1}, and a v_4 asymmetric bending peak at 600−640 cm^{-1}, are

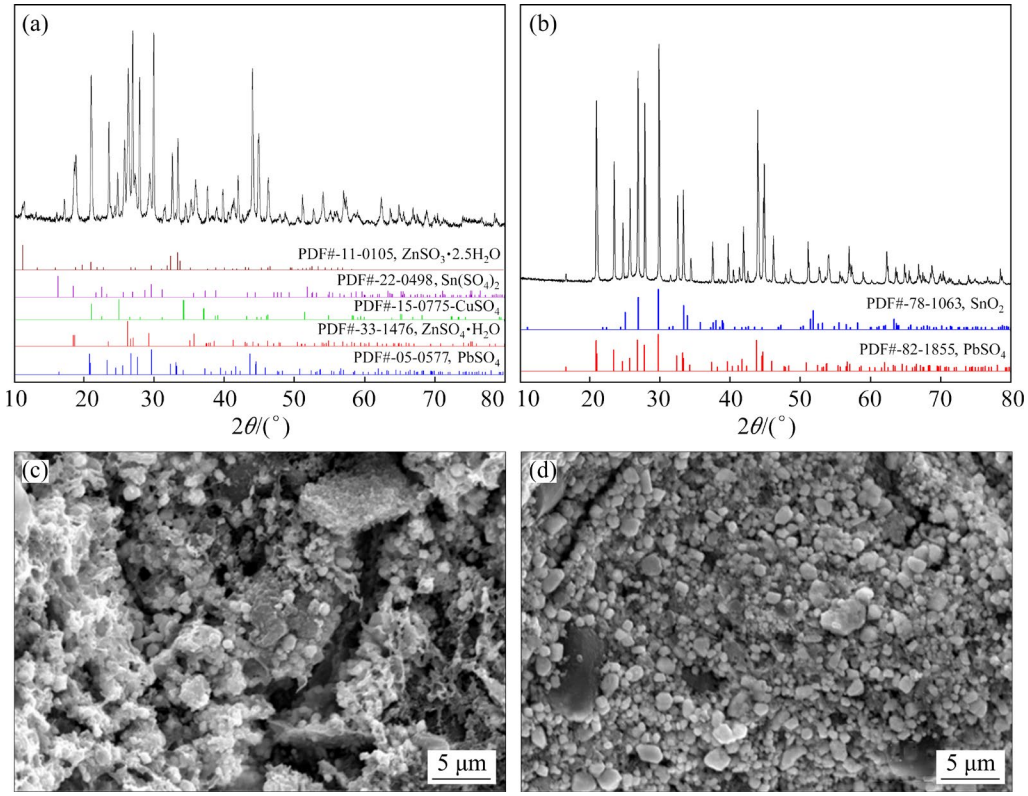

Fig. 4 XRD patterns (a, b) and SEM images (c, d) of roasting product (a, c) and leaching residue (b, d)

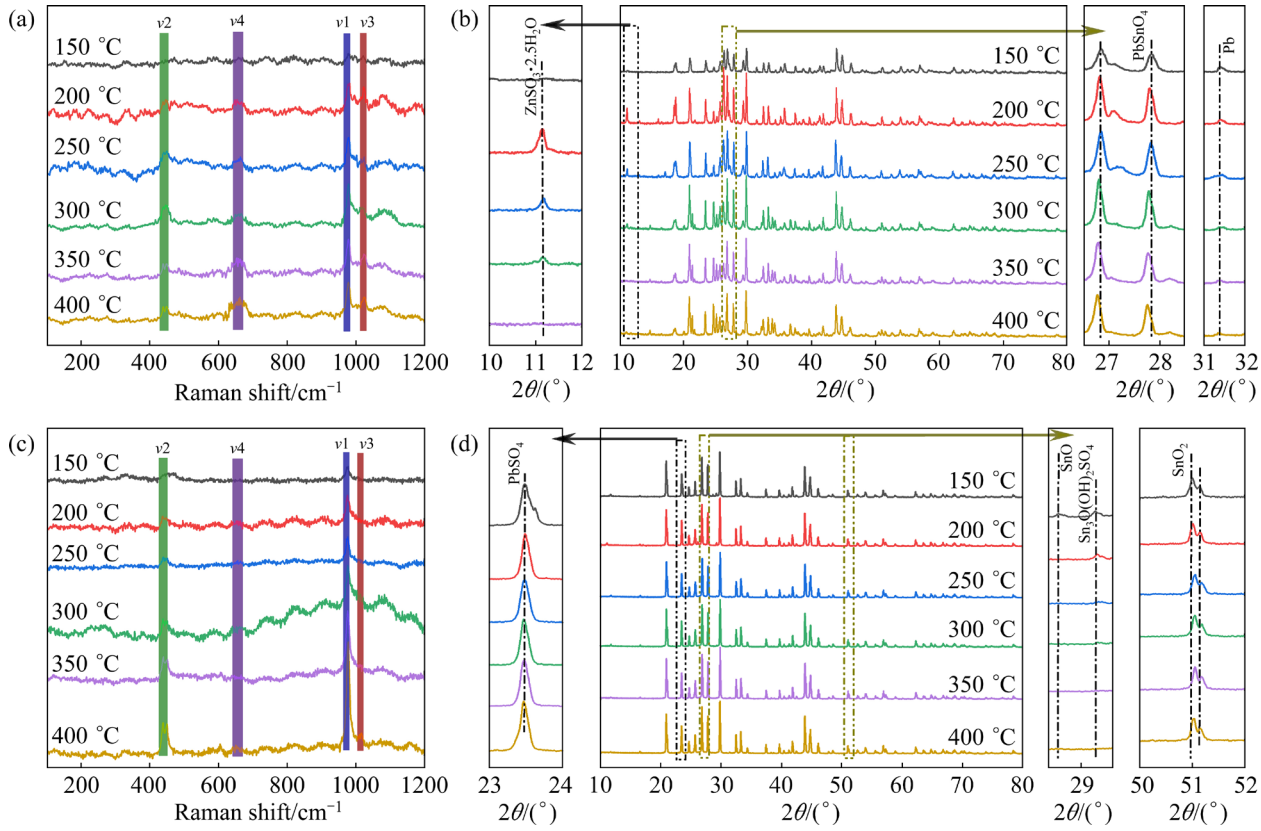

Fig. 5 Raman spectra (a, c) and XRD patterns (b, d) of roasting product (a, b) and leaching residue (c, d) obtained at different roasting temperatures

related to the vibration of the sulfate ion. The intensity of these characteristic peaks increased with increasing the roasting temperature, proving that the degree of crystallinity of metal sulfates increased as the roasting temperature increased. With the increase of the roasting temperature and the dissolution of soluble sulfate, the crystallinity and purity of the metal sulfate in the leaching residues increased, resulting in the formation of a sharp absorption band at 980 cm^{-1}. The Raman results confirm the feasibility from various metal species to the corresponding metal sulfate in the sulfating roasting process.

The structural information of different samples obtained at different roasting temperatures was determined by XRD analysis. As shown in Fig. 5(b), zinc sulfate and lead sulfate are dominant species at any roasting temperature. A weak peak for $ZnSO_3·2.5H_2O$, which is ascribed to the oxidation of ZnS, appeared at 2θ value of 11.2° as the roasting temperature reached 200 °C. The formation of soluble zinc sulfite benefits the recovery of Zn. As the roasting temperature increased, the intensity gradually decreased and finally disappeared. Additionally, the characteristic peak intensity of $PbSO_4$ at 2θ values of 26.8° and 27.8° increased gradually with the increase of the roasting temperatures, accompanied by a weakening of the elemental Pb peak at 2θ value of 31.4°. These results indicate that high temperature promotes the transformation from Pb to $PbSO_4$. From the enlarged data at 2θ values from 26.5° to 28.5°, the characteristic diffraction peaks of $PbSO_4$ exhibit a leftward shift, especially at high roasting temperatures, probably due to the formation of the basic sulphates such as $3PbO·PbSO_4·H_2O$ [36].

As shown in Fig. 5(d), the dominant species in the leaching residue is $PbSO_4$ at all roasting temperatures. When the roasting temperature was 150 °C, a characteristic peak of metallic Sn at 2θ value of 23.6° was observed. This peak disappeared at a roasting temperature of 200 °C. This result suggests the oxidation of tin at high roasting temperatures. Some peaks ascribed to stannous oxide and tin subsulfate emerged at roasting temperatures below 250 °C. The reason for the formation of tin subsulfate is probably the hydrolytic precipitation of soluble tin during the

water leaching process, which is also consistent with the leaching results for Sn shown in Fig. 5(c). The peaks of SnO_2 at 2θ value of approximately 51° gradually shift rightward with increasing temperature, potentially due to the incorporation of other elements [37]. The XRD results show that high temperatures promote the formation of metal sulfates and improve their conversion levels.

A thermal analysis of the SCS dust and concentrated sulfuric acid mixture was conducted using the TG−DSC−MS technique (shown in Supplementary Materials), and the corresponding compositions in the pyrolysis exhaust were recorded in situ using mass spectrometry to further explore the volatilization behaviour of F and Cl in the roasting process. The TG curve in Fig. 6(a) displays three apparent mass loss stages, with temperature ranges of 25−315 °C, 315−650 °C and 650−800 °C, respectively. The DSC results show that the first stage is exothermic, and the latter two stages are endothermic. The in situ MS results for the evolved gas suggest two distinct signals of HF and HCl when the temperature is below 300 °C, and the maximum volatilization rates occur at 190 and 210 °C, respectively. Based on these results, the first mass loss is mainly attributed to the volatilization of HF and HCl. This result also confirms the feasibility of halogen removal for a sulfating roasting temperature of higher than 200 °C. In the second mass loss stage, the peaks of H_2O, SO_2 and SO_3 appear at approximately 390 °C (see Figs. 6(d) and (e) and Fig. S5 in Supplementary Materials), confirming the decomposition of unreacted H_2SO_4. When the roasting temperature reaches over 700 °C, the decomposition of metal sulfate may occur, resulting in the formation of SO_2 at high temperatures. The roasting temperature should be less than 300 °C to avoid the subsequent disposal of SO_2 acid gas.

The roasting products obtained at different temperatures were characterized using XPS to obtain a deeper understanding of the effect of roasting temperature on the sulphation reaction behaviour. As shown in Figs. 7(a) and (b), the characteristic peak intensities of Pb 4f and Zn 2p which are ascribed to Pb(II) and Zn(II) species [38,39] respectively remain unchanged, suggesting the impregnability of the Pb and Zn valence states at different roasting temperatures.

The Sn 3d spectra in Fig. 7(c) are split into two peaks at 486.7 and.487.5 eV, which are attributed to Sn(II) and Sn(IV) [40], respectively. The proportions of Sn(II) and Sn(IV) on the surface of the roasting products were obviously weakened compared with those of the raw dust, and their proportions further decreased as the roasting temperature increased from 150 to 350 °C, suggesting that the roasting temperature benefits the oxidation of Sn(II) species to Sn(IV) species.

After the deconvolution of the Cu 2p spectra, two peaks at 934.2 and 955.2 eV are ascribed to Cu(II) species, and two other peaks at 932.1 and 952.6 eV are attributed to Cu species in the low valence states [41]. The Auger copper line (Cu LMM) was used to identify and distinguish Cu species with the low valence states [42,43]. As presented in Fig. S6 of Supplementary Materials, one main peak at a kinetic energy of 915.5 eV in the Cu LMM spectrum, which is ascribed to Cu(I) species, was observed at roasting temperatures lower than 150 °C. Upon further increasing the roasting temperature, the characteristic peaks of Cu(I) disappeared (see Fig. 7(d)), suggesting that Cu(I) species such as CuCl are completely oxidized

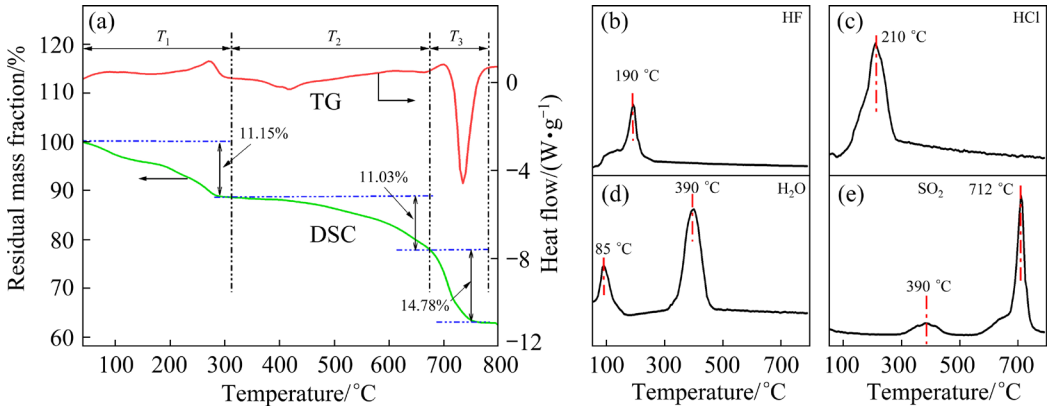

Fig. 6 TG−DSC curves of thermal analysis of SCS dust and sulfuric acid mixture in air at heating rate of 10 °C/min (a), and corresponding MS traces for HF (b), HCl (c), and H_2O (d) and SO_2 (e) in evolved gas

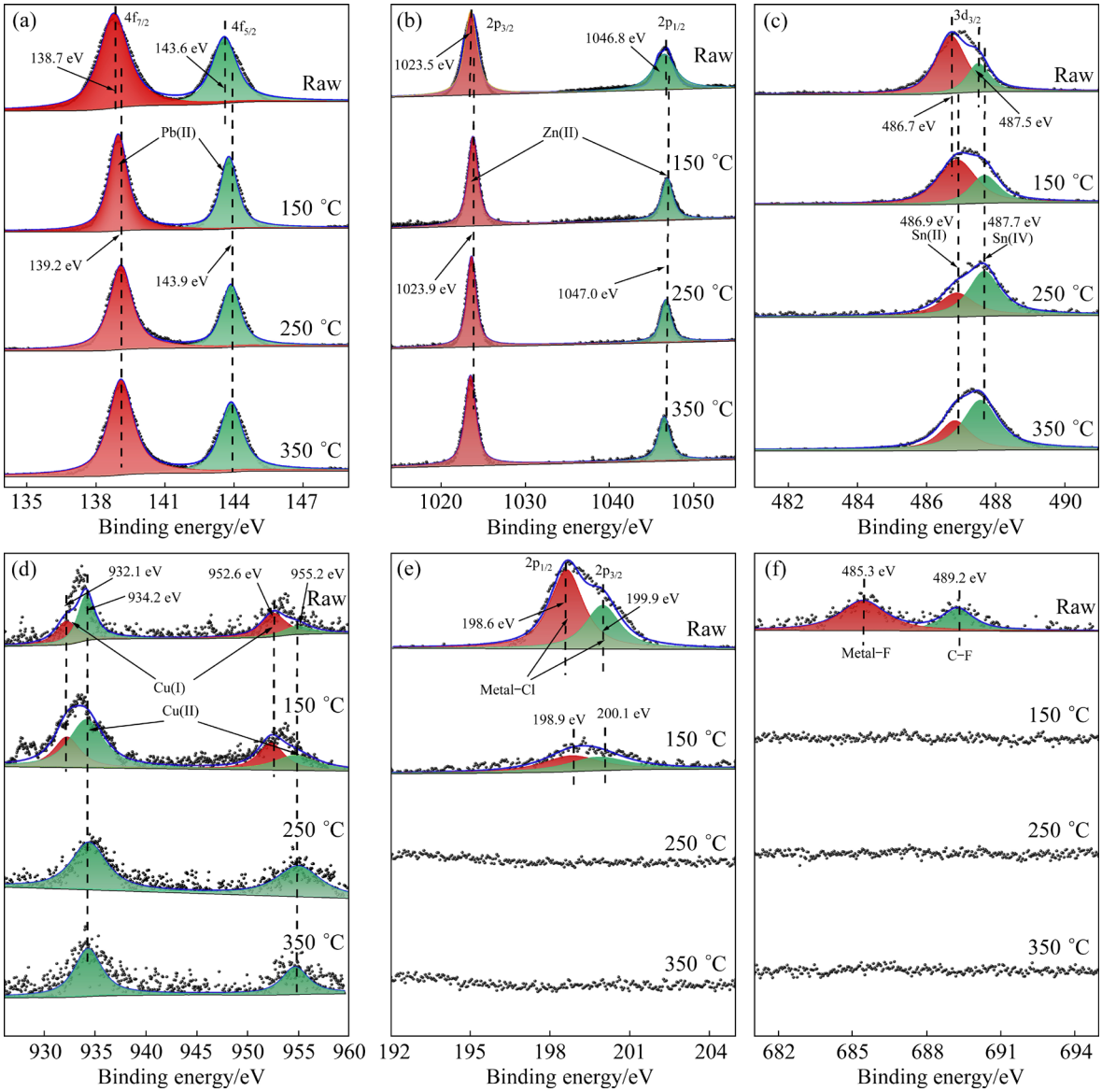

Fig. 7 High-resolution XPS spectra of raw secondary copper smelting dust and roasting products obtained at different roasting temperatures over spectral regions of Pb 4f (a), Zn 2p (b), Sn 3d (c), Cu 2p (d), Cl 2p (e) and F 1s (f)

to Cu(II) species at high temperatures. Combined with the results for the Cu leaching, we conclude that the presence of insoluble Cu(I) species at low roasting temperatures is a major contributor to the low leaching efficiency.

The analysis of the Cl 2p spectrum shown in Fig. 7(e) reveals the presence of peaks for metal chloride at 198.6 and 199.9 eV in the raw dust [44]. Their peak intensities were noticeably reduced for the roasting product obtained at 150 °C and completely disappeared for the roasting products obtained at 250 and 350 °C. In the F 1s spectrum in Fig. 7(f), two characteristic peaks at 485.3 and 489.2 eV emerged for the raw samples, which are ascribed to metal fluoride and fluorinated organic compounds [45]. These characteristic peaks were not detected in all roasting products. The Cl 2p and F 1s spectra obtained at different roasting temperatures indicate that halogens are easily and efficiently removed, especially at high roasting temperatures. Therefore, sulfating roasting is a simple and high-efficiency technology for the efficient separation of halogens from SCS dust.

3.6 Evaluation of feasibility of proposed process

As shown in Fig. 8, the flow sheet of this proposed technology mainly involves four steps, namely, sulfating roasting, water leaching, solvent extraction and mechanochemical reduction. After sulfating roasting and water leaching process, the

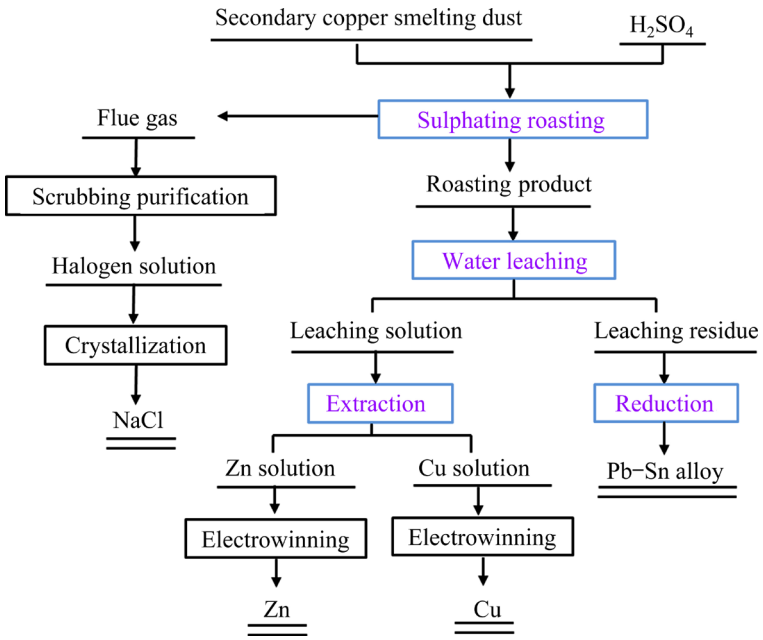

Fig. 8 Flow sheet of proposed technology in this study for treatment of SCS dust

solvent extraction technique was applied to separating Cu and Zn from leaching solution. Two solutions with a Cu concentration of 32.3 g/L and a Zn concentration of 46.8 g/L were finally obtained respectively, which is suitable for yielding metal Zn and Cu products by the electrowinning technique. Finally, mechanochemical reduction was applied to recovering Pb and Sn from the leaching residue in the form of alloy, where the iron powders were used as reducing reagent. The Pb−Sn alloy can be obtained after the removal of residual iron by acid leaching. The total content of Pb and Sn in the obtained alloy is greater than 99.9%. The above analyses suggest the feasibility of this proposed process for the efficient recycle of valuable metals.

A comparison between this proposed process and other technologies reported in literature is presented in Table S4 of Supplementary Materials to further evaluate the overall performance. The results suggest that the proposed technique in this study shows some advantages such as high yield, simple operation, low-cost and high value-added product. Acid leaching is an effective technology for the recovery of copper smelter dust. Cu and Zn can be extracted into leaching solution, while Pb and Bi are enriched in the leaching residue. However, the sulfuric acid leaching results in Table S5 of Supplementary Materials indicate that the Zn and Cu leaching efficiencies are only ~92% and 3.3%, respectively. Meanwhile, approximately 65% of Sn is also leached into solution. The inefficient separation in the acid leaching process brings difficulties to the subsequent metal recovery. The difference of metal species between primary copper smelter dust and secondary copper smelter dust may be the root for the performance difference of acid leaching. Therefore, acid leaching is unsuitable for SCS disposal. Some studies also developed alkaline leaching techniques using NaOH or Na_2CO_3 as leaching agent to recover valuable component from industrial dust. Alkaline leaching techniques require a high alkali charge, namely large leaching solution volume, which will reduce ion concentration in the leaching solution and hence increase the evaporation cost for halogens disposal. A relatively high price of alkali also raises the operating cost. By comparison, sulphating roasting−water leaching is more cost-effective due to the excellent recovery performance and low reagent consumption. What's more, a selective separation of halogens from SCS dust was achieved by this proposed method, which further benefits the subsequent metal separation. Overall, the proposed method is a practicable strategy for the comprehensive recovery of heavy metals and the selective separation of halogens, which also provides a new insight for the recycle of industrial dust containing high-concentration halogen.

4 Conclusions

(1) The thermodynamic calculations confirm the feasibility of transforming various heavy metal species to metal sulfate and harmful halogen elements to gaseous HF and HCl during the sulfating roasting process.

(2) More than 74 wt.% of F and 98 wt.% of Cl evaporate into flue gas during the sulfating roasting process under the optimal conditions (sulfuric acid excess coefficient 1.6, roasting temperature 250 °C, roasting time 30 min and oxygen concentration 20 vol.%).

(3) Water leaching step was used to separate heavy metals, where the leaching efficiencies of Zn and Cu reached higher than 98.6 wt.% and 96.5 wt.% and more than 99.7 wt.% of Pb and Sn remained in the leaching residue.

(4) The mechanism studies show that the roasting temperature accelerates the sulphation reactions from various metal species to metal sulfates and the salting out reactions from various metal halides to gaseous hydrogen halides.

CRediT authorship contribution statement

Zhi-lou LIU: Conceptualization, Methodology, Investigation, Data curation, Writing − Original draft, Writing − Review & editing; **Zhi-kang CHEN:** Methodology, Software, Investigation, Writing − Original draft, Formal analysis; **Fu-ze SUN:** Methodology, Investigation, Data curation; **Zhi-heng ZHANG:** Software, Formal analysis; **Kang YAN:** Formal analysis, Software; **Shui-ping ZHONG:** Investigation, Validation; **Hui LIU:** Supervision, Writing − Review & editing; **Rui-xiang WANG:** Project administration, Funding acquisition, Writing − Review & editing; **Jia-yuan LI:** Supervision, Writing − Review & editing; **Zhi-feng XU:** Writing − Review & editing.

Declaration of competing interest

The authors declare that they have no known competing financial interests or personal relationships that could have appeared to influence the work reported in this paper.

Acknowledgments

This work was supported by the National Key Research and Development Program of China (No. 2019YFC1908400), the National Natural Science Foundation of China (Nos. 52174334, 52374413), the Jiangxi Provincial Cultivation Program for Academic and Technical Leaders of Major Subjects, China (Nos. 20212BCJ23007, 20212BCJL23052), the Jiangxi Provincial Natural Science Foundation, China (Nos. 20224ACB214009, 20224BAB214040), the Double Thousand Plan of Jiangxi Province, China (No. S2021GDQN2970), and the Distinguished Professor Program of Jinggang Scholars in Institutions of Higher Learning of Jiangxi Province, China.

Supplementary Materials

Supplementary Materials in this paper can be found at: http://tnmsc.csu.edu.cn/download/21-p2686-2023-0241-Supplementary_Materials.pdf.

References

[1] OKANIGBE D O, POPOOLA A P I, ADELEKE A A. Characterization of copper smelter dust for copper recovery [J]. Procedia Manufacturing, 2017, 7: 121−126.

[2] SHI Mei-qing, MIN Xiao-bo, SHEN Chen, CHAI Li-yuan, KE YONG, YAN Xu, LIANG Yan-jie. Separation and recovery of copper in Cu−As-bearing copper electrorefining black slime by oxidation acid leaching and sulfide precipitation [J]. Transactions of Nonferrous Metals Society of China, 2021, 31(4): 1103−1112.

[3] ZHANG Xing-fei, YUAN Jia, TIAN Jia, HAN Hai-sheng, SUN Wei, YUE Tong, YANG Yue, WANG Li, CAO Xue-feng, LU Cheng-long. Ultrasonic-enhanced selective sulfide precipitation of copper ions from copper smelting dust using monoclinic pyrrhotite [J]. Transactions of Nonferrous Metals Society of China, 2022, 32(2): 682−695.

[4] JIN Rong, LIU Guo-rui, ZHENG Ming-hui, JIANG Xiao-xu, ZHAO Yu-yang, YANG Li-li, WU Xiao-lin, XU Yang. Secondary copper smelters as sources of chlorinated and brominated polycyclic aromatic hydrocarbons [J]. Environmental Science & Technology, 2017, 51(14): 7945−7953.

[5] ZHAO Kai-xing, HU Yu-yan, TIAN Yu-yi, CHEN De-zhen, FENG Yu-heng. Chlorine removal from MSWI fly ash by thermal treatment: Effects of iron/aluminum additives [J]. Journal of Environmental Sciences, 2020, 88: 112−121.

[6] JIANG Xiao-xu, LIU Guo-rui, WANG Mei, ZHENG Ming-hui. Fly ash-mediated formation of polychlorinated naphthalenes during secondary copper smelting and mechanistic aspects [J]. Chemosphere, 2015, 119: 1091−1098.

[7] RYFA A, ZMUDA R, MANDRELA S, BIALECKI R, ADAMCZYK W, NOWAK M, LELEK L, BANDOLA D, PICHURA M, PLONKA J, WDOWIN M. Experimental and numerical investigation of mercury removal from flue gas by sorbent polymer composite [J]. Fuel, 2023, 333: 126470.

[8] CHEN Jun, ZHANG Wen-juan, MA Bao-zhong, CHE Jian-yong, XIA Liu, WEN Pei-cheng, WANG Chen-yan. Recovering metals from flue dust produced in secondary copper smelting through a novel process combining low temperature roasting, water leaching and mechanochemical reduction [J]. Journal of Hazardous Materials, 2022, 430:

128497.

[9] YU Shi-lin, TAO Run-ze, TAN Hou-zhang, ZHOU Ao, DENG Shuang-hui, WANG Xue-bin, ZHANG Qing-fu. Migration characteristics and ecological risk assessment of heavy metals in ash from sewage sludge co-combustion in coal-fired power plants [J]. Fuel, 2023, 333: 126420.

[10] SABZEZARI B, KOLEINI S M J, GHASSA S, SHAHBAZI B, CHEHREH C S. Microwave−leaching of copper smelting dust for Cu and Zn extraction [J]. Materials, 2019, 12(11): 1822.

[11] YU Xiao-qiang, XU Jia-cong, YI Qin, WEN Sheng-hui, TIAN Lei. Study on separating arsenic and antimony by NaOH alkali leaching of arsenic and antimony soot [J]. Nonferrous Metals Science and Engineering, 2021, 12(3): 42−49. (in Chinese)

[12] SHAHNAZI A, FIROOZI S, HAGHSHENAS D. Selective leaching of arsenic from copper converter flue dust by Na_2S and its stabilization with $Fe_2(SO_4)_3$ [J]. Transactions of Nonferrous Metals Society of China, 2020, 30(6): 1674−1686.

[13] ZHANG Er-jun, ZHOU Kang-gen, CHEN Wei, ZHANG Xue-kai, PENG Chang-hong. Separation of As and Bi and enrichment of As, Cu, and Zn from copper dust using an oxidation-leaching approach [J]. Chinese Journal of Chemical Engineering, 2021, 33: 125−131.

[14] LIU Zhi-lou, ZHANG Zhi-heng, LI Zi-liang, XIE Xiao-feng, ZHONG Shui-ping, LI Yu-hu, XU Zhi-feng, LIU Hui. 3D hierarchical iron−cobalt sulfide anchored on carbon fiber with abundant active short chain sulfur for high-efficiency capture of elemental mercury [J]. Chemical Engineering Journal, 2021, 418: 129442.

[15] BAKHTIARI F, ATASHI H, ZIVDAR M, SEYEDBAGHERI S, FAZAELIPOOR M H. Bioleaching kinetics of copper from copper smelters dust [J]. Journal of Industrial and Engineering Chemistry, 2011, 17(1): 29−35.

[16] JEON S, TABELIN C B, TAKAHASHI H, PARK I, ITO M, HIROYOSHI N. Enhanced cementation of gold via galvanic interactions using activated carbon and zero-valent aluminum: A novel approach to recover gold ions from ammonium thiosulfate medium [J]. Hydrometallurgy, 2020, 191: 105165.

[17] KUMAR M, NANDI M, PAKSHIRAJAN K. Recent advances in heavy metal recovery from wastewater by biogenic sulfide precipitation [J]. Journal of Environmental Management, 2021, 278: 111555.

[18] LI Cun-xiao, ZHANG Zhao-yan, ZHANG Yao-yang, DENG Zhi-gan, JI Wen-bin, LIN Xiao-tan. Reductive leaching kinetics of indium and further selective separation by fraction precipitation [J]. Transactions of Nonferrous Metals Society of China, 2023, 33(1): 315−324.

[19] KUBOTA F, KONO R, YOSHIDA W, SHARAF M, KOLEV S D, GOTO M. Recovery of gold ions from discarded mobile phone leachate by solvent extraction and polymer inclusion membrane (PIM) based separation using an amic acid extractant [J]. Separation and Purification Technology, 2019, 214: 156−161.

[20] LI Zi-liang, XU Zhi-feng, ZHANG Xi, ZAN Miao-miao, LIU Zhi-lou. Mercury recovery from acidic mercury solution using electrodeposition [J]. Chinese Journal of Engineering, 2020, 42(8): 999−1006. (in Chinese)

[21] LIU Zhi-lou, WANG Dong-li, YANG Shu, LIU Hui, LIU Cao, XIE Xiao-feng, XU Zhi-feng. Selective recovery of mercury from high mercury-containing smelting wastes using an iodide solution system [J]. Journal of Hazardous Materials, 2019, 363: 179−186.

[22] WANG Xiao-na, WANG Meng-lu, ZOU De-zhi, WU Chuan-fu, LI Teng, GAO Ming, LIU Shu, WANG Qun-hui, SHIMAOKA T. Comparative study on inorganic Cl removal of municipal solid waste fly ash using different types and concentrations of organic acids[J]. Chemosphere, 2020, 261: 127754.

[23] YE Lei, PENG Zhi-wei, YE Qing, WANG Lian-cheng, AUGUSTINE R, PEREZ M, LIU Yong, TANG Hui-min, RAO Ming-jun, LI Guang-hui, JIANG Tao. Toward environmentally friendly direct reduced iron production: A novel route of comprehensive utilization of blast furnace dust and electric arc furnace dust [J]. Waste Management, 2021, 135: 389−396.

[24] XU Bin, MA Yong-peng, GAO Wei, YANG Jun-kui, YANG Yong-bin, LI Qian, JIANG Tao. A review of the comprehensive recovery of valuable elements from copper smelting open-circuit dust and arsenic treatment [J]. JOM, 2020, 72(11): 3860−3875.

[25] ZHONG Da-peng, LI Lei. Separation of arsenic from arsenic−antimony-bearing dust through selective oxidation−sulfidation roasting with CuS [J]. Transactions of Nonferrous Metals Society of China, 2020, 30(1): 223−235.

[26] CHEN W S, SHEN Y W, TSAI M S, CHANG F C. Removal of chloride from electric arc furnace dust [J]. Journal of Hazardous Materials, 2011, 190(1): 639−644.

[27] CHEN W, KIRKELUND G M, JENSEN P E, OTTOSEN L M. Comparison of different MSWI fly ash treatment processes on the thermal behavior of As, Cr, Pb and Zn in the ash [J]. Waste Management, 2017, 68: 240−251.

[28] MA Wen-chao, HOFFMANN G, SCHIRMER M, CHEN Guan-yi, ROTTER V S. Chlorine characterization and thermal behavior in MSW and RDF [J]. Journal of Hazardous Materials, 2010, 178(1/2/3): 489−498.

[29] YANG S, SAFFARZADEH A, SHIMAOKA T, KAWANO T. Existence of Cl in municipal solid waste incineration bottom ash and dechlorination effect of thermal treatment [J]. Journal of Hazardous Materials, 2014, 267: 214−220.

[30] LIU Zhi-lou, WANG Dong-li, PENG Bing, CHAI Li-yuan, LIU Hui, YANG Shu, YANG Ben-tao, XIANG Kai-song, LIU Cao. Transport and transformation of mercury during wet flue gas cleaning process of nonferrous metal smelting [J]. Environmental Science and Pollution Research, 2017, 24: 22494−22502.

[31] CALVO G, MUDD G, VALERO A, VALERO A. Decreasing ore grades in global metallic mining: A theoretical issue or a global reality? [J]. Resources, 2016, 5(4): 36.

[32] ZHANG Zheng-hua, ZHU Xiang-dong, HOU Hhui-liang, TANG Lei, XIAO Jin, ZHONG Qi-fan. Regeneration and utilization of graphite from the spent lithium-ion batteries by modified low-temperature sulfuric acid roasting [J]. Waste Management, 2022, 150: 30−38.

[33] LI Peng-wei, LUO Shao-ua, FENG Jian, LV Fang, YAN Sheng-xue, WANG Qing, ZHANF Ua-hui, MU Wen-ning,

LIU Xin, LEI Xue-fei, TENG Fei, LI Xian, CHANG Long-jiao, LIANG Jin-sheng, DUAN Xin-hui. Study on the high-efficiency separation of Fe in extracted vanadium residue by sulfuric acid roasting and the solidification behavior of V and Cr [J]. Separation and Purification Technology, 2021, 269: 118687.

[34] QIU Yang-bo, REN Long-fei, SHAO Jia-hui, XIA Lei, ZHAO Yan. An integrated separation technology for high fluoride-containing wastewater treatment: Fluoride removal, membrane fouling behavior and control [J]. Journal of Cleaner Production, 2022, 349: 131225.

[35] FANG Ping, TANG Zi-jun, CHEN Xiong-bo, HUANG Jian-hang, TANG Zhi-xiong, CEN Chao-ping. Chloride ion removal from the wet flue gas desulfurization and denitrification wastewater using Friedel's salt precipitation method [J]. Journal of Chemistry, 2018, 2018: 5461060.

[36] ANGERER P, MANN R, GAVRILOVIC A, NAUER G. In situ X-ray diffraction study of the electrochemical reaction on lead electrodes in sulphate electrolytes [J]. Materials Chemistry and Physics, 2009, 114(2/3): 983−989.

[37] JIN W X, MA S Y, TIE Z Z, WEI J J, LUO J, JIANG X H, WANG T T, LI W Q, CHENG L, MAO Y Z. One-step synthesis and highly gas-sensing properties of hierarchical Cu-doped SnO_2 nanoflowers [J]. Sensors and Actuators B: Chemical, 2015, 213: 171−180.

[38] LONG Hai-lin, LI Hao-yu, MA Peng-cheng, ZHOU Zhu-fen, XIE Hui-min, YIN Shao-hua, WANG Yong-mi, ZHANG Li-bo, LI Shi-wei. Effectiveness of thermal treatment on Pb recovery and Cl removal from sintering dust [J]. Journal of Hazardous Materials, 2021, 403: 123595.

[39] XIE Xiao-feng, ZHANG Zhi-heng, CHEN Zhi-kang, WU Ji-yao, LI Zi-liang, ZHONG Shui-ping, LIU Hui, XU Zhi-feng, LIU Zhi-lou. In-situ preparation of zinc sulfide adsorbent using local materials for elemental mercury immobilization and recovery from zinc smelting flue gas [J]. Chemical Engineering Journal, 2022, 429: 132115.

[40] ZHAO Hui, SUN Xu, HAO Long, WANG Jian-qiu, YANG Jing-mei. Corrosion evolution of high-temperature formed oxide film on pure Sn solder substrate [J]. Transactions of Nonferrous Metals Society of China, 2022, 32(12): 3998−4013.

[41] YANG Shu, WANG Dong-li, LIU Hui, LIU Cao, XIE Xiao-feng, XU Zhi-feng, LIU Zhi-lou. Highly stable activated carbon composite material to selectively capture gas-phase elemental mercury from smelting flue gas: Copper polysulfide modification [J]. Chemical Engineering Journal, 2019, 358: 1235−1242.

[42] SU Kai, JI Yong-jun, ZHOU Xi-wen, JIANG Xing-yu, LI Hui-fang, ZHU Yong-xia, LI Jiang, LIU He-zhi, XIAO Jun-ping, ZHONG Zi-yi. Approach to generating the right active phase in the "Direct" synthesis of trimethoxysilanes using the CuCl−Cu_2O catalyst [J]. Applied Surface Science, 2021, 544: 148915.

[43] YANG Shu, LIU Zhi-lou, YAN Xu, LIU Cao, ZHANG Zi-yan, LIU Hui, CHAI Li-yuan. Catalytic oxidation of elemental mercury in coal-combustion flue gas over the $CuAlO_2$ catalyst [J]. Energy & Fuels, 2019, 33(11): 11380−11388.

[44] FAN Meng-jie, ZOU Qing-ping, LIU Ji-ning, CHEN Ying-wen, ZHU Jian-liang, SHEN Shu-bao. Enhanced catalytic oxidation of dichloromethane by a surfactant-modified CeO_2@TiO_2 core–shell nanostructured catalyst [J]. Journal of Rare Earths, 2023, 41(7): 1031−1041.

[45] YANG Yu-sheng, WANG Tuo-yao, ZHAO Ran, ZHANG Shu-yan, ZHAO Zeng-wu. Molten salt synthesis of neodynium oxyfluoride in various fluoride media with different fluoride ion activities [J]. Journal of Rare Earths, 2022, 40(12): 1935−1944.

再生铜烟灰中卤素的分离和重金属的回收

刘志楼[1]，陈志康[1]，孙辅泽[1]，张志恒[1]，严 康[1]，衷水平[1]，刘 恢[1]，王瑞祥[1]，李家元[2]，徐志峰[3,4]

1. 江西理工大学 冶金工程学院，赣州 341000；
2. 湘南学院 化学与环境科学学院，郴州 423000；
3. 赣州市绿色冶金与工艺强化工程技术研究中心，赣州 341000；
4. 自然资源部 离子稀土资源与环境重点实验室，赣州 341000

摘 要：采用硫酸化焙烧−水浸工艺对再生铜烟灰中卤素分离和重金属回收进行研究。热力学结果证实了物相向硫酸盐和气态 HF 和 HCl 转化的可行性。在硫酸化焙烧温度 250 ℃和硫酸过量系数 1.8 的反应条件下，超过 74%(质量分数)的 F 和 98%(质量分数)的 Cl 挥发进入烟气。经过水浸后，焙烧产物中约 98.6%(质量分数)的 Zn 和 96.5%(质量分数)的 Cu 溶解到浸出液中，而 Pb 和 Sn 的浸出率分别仅为 0.12%和 0.22%。机制研究结果表明，焙烧温度对金属化合物向金属硫酸盐的硫酸化反应和金属卤化物向气态卤化氢的盐析反应起到重要作用。

关键词：再生铜烟灰；硫酸化焙烧；水浸；卤素挥发；重金属分离

(Edited by Wei-ping CHEN)